KeAi
CHINESE ROOTS
GLOBAL IMPACT

Available online at www.sciencedirect.com

ScienceDirect

Advances in Climate Change Research 9 (2018) 170–176

www.keaipublishing.com/en/journals/accr/

Changes of tropical cyclone tracks in the western North Pacific over 1979–2016

ZHANG Wen-Qian[a], WU Li-Guang[a,*], ZOU Xu-Kai[b]

[a] *Pacific Typhoon Research Center, Nanjing University of Information Science & Technology, Nanjing 210044, China*
[b] *Key Laboratory for Climate Studies National Climate Center, China Meteorological Administration, Beijing 100081, China*

Received 28 February 2018; revised 26 April 2018; accepted 15 June 2018
Available online 23 June 2018

Abstract

The tropical cyclone (TC) trajectory model has been widely used to investigate the mechanism of the climate change of TC tracks. In this study, the Gaussian weight interpolation method is used to calculate the beta drift in the TC track or trajectory model. By simulating historical TC tracks, the new calculation can better simulate the spatial distribution of the frequency of TC occurrence. The improved track model is further used to understand the TC track change during the period of 1979–2016. In 1979–2016, the TC activity has been suppressed in the South China Sea (SCS) while the TC influence along the southeast coastal regions of China has been increased. The sensitivity experiments indicate that the change of the formation location plays a dominant role in decreasing TC influence in the SCS while the change of the environmental steering flows increases the TC influence in the eastern coastal region of China. This study suggests that the ongoing climate change can affect the TC activity along the coast of China.

Keywords: Tropical cyclone; Trajectory model; Beta drift; Formation position; Large-scale steering flows

1. Introduction

The western North Pacific (WNP) is the most active area for tropical cyclones (TCs) in the world, which cause tremendous losses in life and property in the coastal areas of China (Chen and Meng, 2001; Zhang et al., 2009, 2011). The beneficial aspect is that TC precipitation can mitigate drought in arid regions (Sugg, 1968). The change of TC tracks not only leads to the shift of the TC influence area but also changes TC intensity because of the changing environmental fields that TCs experience. The research on the climate change of TC tracks in the western North Pacific is of practical importance, providing a scientific basis for the seasonal forecast of TC tracks in the western North Pacific and guiding the government through prevention and mitigation of TC disasters.

Studies on TC climate change need a large sample size to obtain reliable results. In this case, a trajectory model is often used to augment the sample size in TC tracks. There are two types of TC trajectory models with the major difference in the calculation of TC motion velocity. One is based on historical TC records using statistical methods to calculate the velocity (Hall and Jewson, 2007; Yonekura and Hall, 2011, 2014). The other is based on two fundamental mechanisms for TC motion. TC translation velocity is the sum of the large-scale environmental steering flow and the beta drift (Wang et al., 1998). Using the first type of the trajectory models, the influence of ENSO on TC tracks can be simulated based on historical TC formation positions and translation velocities (Yonekura and Hall, 2011, 2014). Although this type of trajectory models can adjust TC propagation by Nino3.4 index averaged over July–October, it cannot be used to downscale the future change of TC tracks. The second type of the track models can simulate historical TC tracks, and estimate the influence of global warming on TC tracks (Wu and Wang, 2004; Wu et al.,

* Corresponding author.
E-mail address: liguang@nuist.edu.cn (WU L.-G.).
Peer review under responsibility of National Climate Center (China Meteorological Administration).

https://doi.org/10.1016/j.accre.2018.06.002

2005; Emanuel et al., 2006; Zhao et al., 2010; Zhao and Wu, 2014; Wang and Wu, 2015). The estimation of the beta drift varies in different studies. Wu and Wang (2004) use the climatologic beta drift calculated from best track data at each 2.5° × 2.5° grid point. Emanuel et al. (2006) set the beta drift a constant value ($v = 2.5$ m s^{-1}, $u = 0$ m s^{-1}) for the whole basin. Zhao et al. (2009) used a relationship between climatologic beta drift and large-scale environmental steering flow (Zhao et al., 2010; Zhao and Wu, 2014; Wang and Wu, 2015).

A TC track is determined mainly by its initial location and the subsequent movement. The initial location means where a TC forms. Studies focus mainly on the influence of large-scale environmental flows on TC genesis using observation data or genesis potential index (GPI) (Wang and Chan, 2002; Murakami et al., 2011; Zhao et al., 2012; Wang and Wu, 2013, 2016; Wu et al., 2015). For example, Wu and Wang (2004) shifted all the locations of TC formation to examine the influence of the initial location on TC tracks. They found that TC tracks can be affected by the formation position and this influence is larger than that of large-scale steering flows. But further studies found that the change of large-scale steering flows plays a more important role than TC formation locations in the inter-decadal change or ENSO influence of TC tracks (Zhao et al., 2010; Zhao and Wu, 2014).

The change of TC tracks can be explained well just by the change of large-scale steering flows (Wu and Wang, 2004; Ho et al., 2004; Wu et al., 2005; Wang et al., 2009a; Colbert and Soden, 2012). Wu et al. (2005) explain the westward shift of two prevailing tracks in WNP by the change of steering flows. The change of prevailing tracks increases TC influence over eastern China but decrease the influence in the South China Sea (SCS). Under the Representative Concentration Pathway 4.5 (RCP4.5) scenario, the westward shifting will continue by downscaling a selection of nine CMIP5 climate models (Wang and Wu, 2015). Analyzing landfall data in China can obtain a similar result. There is a decrease in the number of landfall TCs in the coastal area to the south of Xiamen and an increase to the north with an intensification for the whole area (Wang et al., 2009b; Yang et al., 2009).

The trajectory model using large-scale environmental steering flows and the beta drift is better than the statistical trajectory model since the former is based on the dynamics of TC motion. However, different ways to calculate the beta drift can affect the simulation results. A new method is used in this study to calculate the beta drift, and the climate change of TC tracks over WNP during the past 38 years (1979–2016) is examined by using the improved model. Then we design numerical experiments to evaluate the relative contributions of changes in the large-scale environmental steering flow and formation locations, respectively.

2. Data

The TC best track dataset used in this study is from the Joint Typhoon Warming Center (JTWC), including the TC location, the one-minute maximum sustained wind speed, and the central pressure at 6-h intervals. In the 1960s satellites began to monitor TCs, and by the 1970s it can be safely assumed that hardly any TC events were missed (Emanuel, 2008). At the same time, the application of Dvorak technology also makes the estimation of TC intensity more accurate (Liu et al., 2008). Considering the reliability of the TC data, we focus on the peak season (June–October) during 1979–2016. There are 705 TCs that reached at least tropical storm (TS) intensity (1-min averaged maximum sustained wind speed $\geq$ 17.2 m s^{-1}). The location where a TC first reached the TS intensity is taken as the formation position.

The monthly mean wind fields from the National Centers for Environmental Prediction/National Center for Atmospheric Research (NCEP/NCAR) on a 2.5° × 2.5° grid are used (Kalnay et al., 1996). The large-scale steering flow is defined as the pressure-weighted mean flow from 850 to 300 hPa (Holland, 1983), and is averaged over June–October each year in this study. The frequency of TC occurrence and TC formation are calculated in each box of 2.5° × 2.5°(Wu et al., 2005).

3. Improvement in the trajectory model

In the trajectory model, a TC is treated as a point vortex that moves from its formation position at a velocity that includes the large-scale steering flow and the beta drift. The TC motion is terminated until it moves out of the specified area (100°E–180°E, 0°–50°N) or 12 h after landfall.

When we calculate climatologic mean beta drift, the more the samples are used, the more it can represent the climatologic mean state. Due to the limitation of the TC data, the TC records are not evenly distributed. Previous studies first represented the WNP basin with 2.5° × 2.5° grid boxes and calculated the mean translation velocity based on TCs that enter a box (Wu and Wang, 2004; Wu et al., 2005; Zhao et al., 2009). The mean steering flow is subtracted from translation velocity to obtain climatologic mean beta drift. In the calculation of mean translation velocity, the number of samples in each grid must exceed a threshold, so the translation velocity can represent a climatologic mean state. As a result, the calculated beta drift cannot cover the entire WNP basin.

In order to obtain the best beta drift at any position during the simulation, we considered each TC record as a "station", and calculate the translation velocity of the record. Finally, we got 14,828 records of translation velocity with latitudes and longitudes.

According to the previous calculation method of the beta drift, we use the Gaussian weighted interpolation to calculate TC mean translation velocity. Then we can obtain climatologic mean beta drift by subtracting mean steering flow averaged over 1979–2016 at the same position. In the track simulation, the Gaussian interpolation is performed by taking the distance between each record point and the TC center as a weight to calculate the TC velocity:

$$u(q) = \frac{\sum_{i=1}^{14828} u_i \exp\left(-\frac{d_i^2}{2L^2}\right)}{\sum_{i=1}^{14828} \exp\left(-\frac{d_i^2}{2L^2}\right)}, \quad (1)$$

$$v(q) = \frac{\sum_{i=1}^{14828} v_i \exp\left(-\frac{d_i^2}{2L^2}\right)}{\sum_{i=1}^{14828} \exp\left(-\frac{d_i^2}{2L^2}\right)}, \quad (2)$$

where $u(q)$ is the zonal component of TC mean translation velocity at the position q during the simulation; u_i is the zonal component of TC translation velocity calculated by the ith record; d_i is the distance between the ith record and the position q. L is the length scale of the Gaussian weighted interpolation, taken as a constant. $v(q)$, the meridional component of TC mean translation velocity, can be obtained in a similar way.

It can be seen in Eq. (1) that the interpolated results will be different with different length scales, which will affect the simulation in the trajectory model. In order to find the optimal value of L, we introduce an average 6-h forecast error in test simulations. Here we take historical position p_j of a TC record as formation position, then simulate a 6-h position p_j' using the trajectory model. We compute the average of the 6-h forecast error, $\sum_{j=1}^{n}|p_{j+1} - p_j'|/n$, $n = 14828$, which is the distance between the simulated position p_j' and historical position p_{j+1} averaged over all record points of all TCs except the last record of each track during 1979–2016. When we calculate 6-hr forecast errors, the formation position p_j is also the position of translation velocity calculated with the same record. Due to the Gaussian interpolation method, a larger weight of translation velocity calculated by the same record (the value of d_i is as small as possible) will lead to a smaller error and a fake error for normal simulation of a whole track. So the translation velocity calculated with the same record does not participate in the calculation of the Gaussian weight interpolation, when $q = p_j$, $i \neq j$ in Eq. (1). This can more accurately reflect the error of the trajectory model. Fig. 1 shows the mean 6-h forecast error as a function of L by taking 20–1000 km for L. The mean 6-h forecast error first decreases and then increases with an increase of L. When the L value is 120 km, the mean 6-h forecast error reaches the minimum value of 80.9 km. So $L = 120$ km is taken for the following simulation.

In order to compare with the previous method, using the Gaussian interpolation method we compute climatologic beta drifts in 2.5° × 2.5° grid boxes over the period 1979–2016 (Fig. 2a). The climatologic beta drift has a mean orientation of 319° and a mean magnitude of 3.2 m s^{-1}, which are comparable well with Wu and Wang (2004) and Zhao et al. (2009). The mean orientation of the beta drift was 303° with a mean magnitude of 3.0 m s^{-1} in Wu and Wang (2004), and 320° with a mean magnitude of 3.3 m s^{-1} in Zhao et al. (2009). In Fig. 2b, the climatologic beta drift calculated with the previous method is an average over the grid boxes with the sample size exceeding 40 (Zhao et al., 2009). The climatologic beta drift calculated with the Gaussian interpolation method can cover a larger area including 291 grid boxes, compared with 129 grid boxes in the previous method. When there is no values of the beta drift during the TC track simulation, the beta drift averaged over the whole WMP basin is used in previous trajectory model. In the current method, the beta drift at any position can be calculated. So the improved trajectory model can get more accurate beta drifts, especially at coastal areas and higher latitudes.

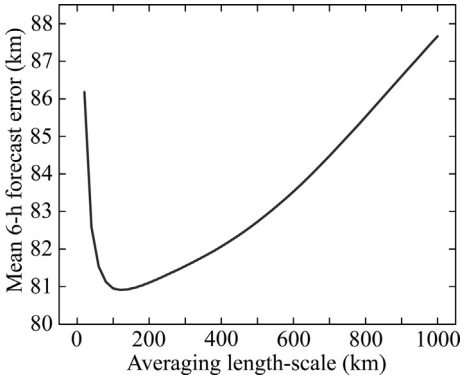

Fig. 1. Mean 6-h forecast error versus averaging length-scale of the Gaussian weighted interpolation.

4. Simulation of tropical cyclones

4.1. Climatology of TC motion

Using the monthly mean large-scale steering flow each year, we simulate June–October TC tracks during 1979–2016, with the original and improved trajectory models, respectively. Fig. 3a shows the spatial distribution of the climatologic mean frequency of TC occurrence based on the JTWC dataset. TCs occur most frequently over the Philippine Sea and the active area extends to the northern South China

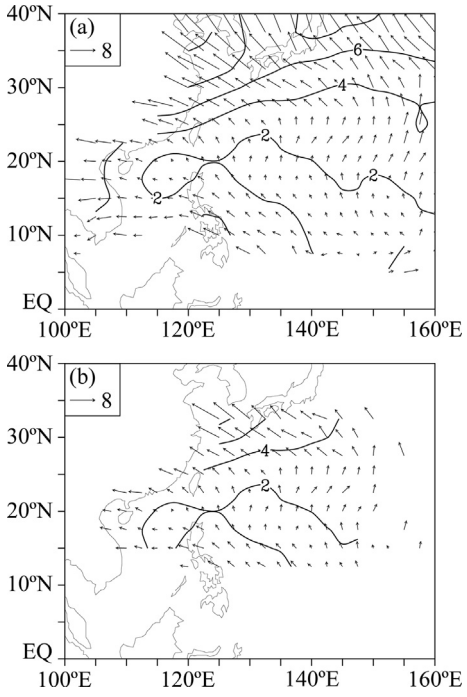

Fig. 2. Climatologic beta drift (vectors) averaged over 1979–2016, (a) is calculated by Gaussian weighted interpolation, (b) is averaged in grid boxes. Contours show the magnitude of beta drift with intervals 2 m s^{-1}.

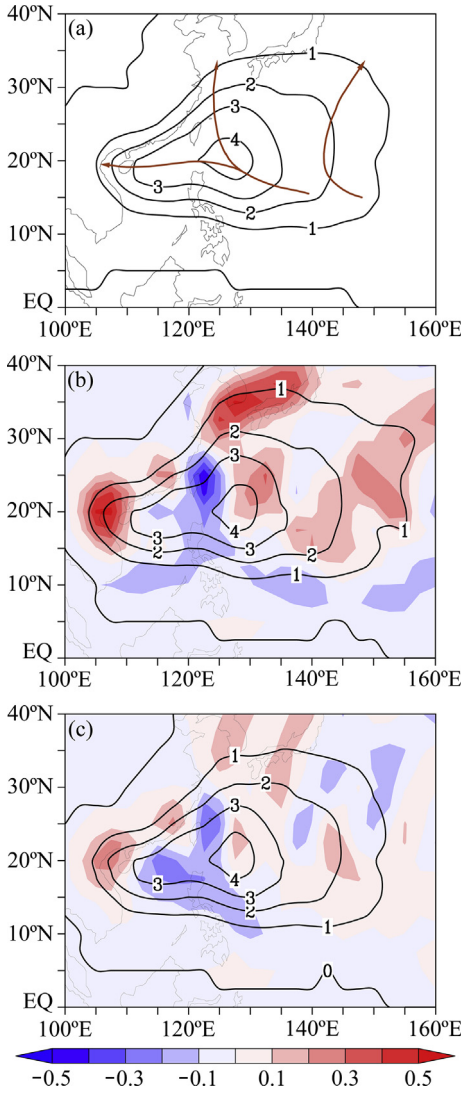

Fig. 3. Spatial distributions of the frequency of TC occurrences in TC peak season (June–October) during 1979–2016 for (a) observation form JTWC, (b) simulation from the model Wu et al. (2005) used, and (c) simulation from the improved model with averaging length-scale of 120 km. Shading in (b) and (c) denotes the difference between simulation and observation. Brown arrows show the climatological typhoon prevailing tracks. The contour intervals are 1 per year.

Sea (SCS). Fig. 3b and c are the comparisons of the simulated climatologic mean frequency of TC occurrence and the corresponding difference between the simulation and observation. In both of the models, the simulated patterns in the frequency of TC occurrence are very similar to the observation (Fig. 3a). We can see that in the improved model the difference between the simulation and observation is significantly reduced in magnitude although there are negative biases in the surrounding of Taiwan and the SCS.

The spatial distribution in the mean bias indicates that the improved model has a better performance. The bias decreases to about half over the western SCS, to the west of Japan and in the vicinity of Taiwan Island. The strong positive anomalies in the original model are replaced by a few weak positive and negative anomalies over the ocean east of 130°E. To verify the optimal value of length scale L, average errors are calculated from simulations setting L to 20–1000 km. The results are the same as shown in Fig. 1. The average errors decrease first and then increases with L increasing. The length of 120 km is also the optimal value of L.

4.2. Climate change of TC tracks

Previous studies have found that the TC influences have decreased in the SCS over the past several decades while the two northward prevailing tracks in the WNP shifted westward, resulting in an increase in the frequency of TC occurrence from the Philippine Sea to the eastern coast of China and a decrease in the eastern part of the WNP (Wu et al., 2005). As shown in Fig. 4a, these changes are also seen during 1979–2016. There are increasing trends around Taiwan Island, Japan and to its south, while the trend in the SCS shows a significant decrease. The simulation in the improved model also shows the similar decreasing influence in the SCS and increasing influence around Taiwan Island and to the southeast of Japan (Fig. 4b). As shown in Fig. 4b, the change in large-scale steering flows is characterized by a cyclonic circulation centered over southeastern China. The enhanced westerly steering flow in the SCS tends to shift TCs northward. The anomalous southeasterly steering flow to the east of Taiwan Island leads to a northward movement of TCs that makes the influence of TCs increase around Taiwan Island. Although the change of steering flow is a good explanation of the TC track

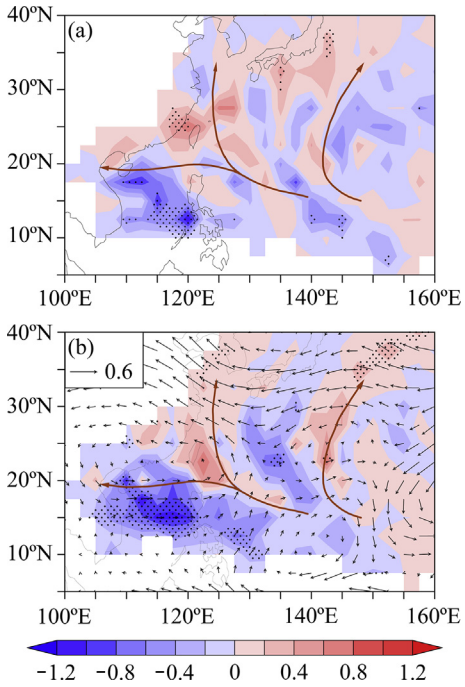

Fig. 4. Linear trend (shading, unit: per decade) of the frequency of TC occurrences and of large-scale steering flows (vectors, unit: m s^{-1} per decade) in TC peak season (June–October) during 1979–2016 for (a) observation from JTWC, (b) simulation from improved model. The trend with dots indicates that the value is statistically significant at 90% confidence level. Brown arrows show the climatological typhoon prevailing tracks.

change over the SCS and the coastal area of China, it cannot explain the change over the WNP since there is also a change in the formation location, which will be discussed in the next section.

5. Influences of changes in environmental steering and formation locations

In order to explore individual influences of changes in the formation location and environmental steering on TC tracks, we design two experiments by holding the formation location or steering flow fixed, respectively, and compare the results with that in the control experiment (E0). All TC tracks of these experiments are simulated by improved trajectory model with $L = 120$ km. The first experiment (E1) is to examine the influence of the change of the formation location by holding the environmental steering flow fixed. The second experiment (E2) is to examine the influence of the change of the environmental steering flow by holding the formation location fixed. In E1, the steering flows averaged over 1979–2016 are used for each year. In E2, the formation location includes those TCs that formed during the period of 1979–2016. That is, all of the formation locations of 705 TCs during 1979–2016 are used for each year as climatologic formation positions. In order to keep the same number of formation locations in E0 and E1, we use the random sampling from a discrete distribution to increase the number of formations according to the TC genesis distribution in $1° \times 1°$ grid boxes each year. The method can maintain the spatial distribution of the TC formation and create 705 formation locations each year.

Fig. 5 shows the comparison of the spatial distribution of TC formation during the period 1979–2016 between the observation (Fig. 5a) and the formation by random sampling (Fig. 5b). We can see that the spatial patterns (contours) derived by the random sampling method are very similar to those from the observation. TCs most frequently form to the east of the Philippines between 10° and 20°N with a second maximum in the SCS. In Fig. 5, we also plot the linear trend of the frequency of TC formation during the period 1979–2016. Such a distribution of the change of TC formation is somewhat similar to that during La Niña years (Wang and Chan, 2002; Zhao et al., 2012). The TC formation is suppressed in the eastern part of the WNP and increasing TC formation can be found west of 130°E. The TC formation in the middle and southern parts of the SCS is also suppressed. It is clear that the sampling method can well produce the changing trend. Therefore, we can identify the individual influences of the changes in the environmental steering and formation locations in E1 and E2 by comparing with the control experiment (E0). Note that the environmental steering and formation locations vary each year. The annual frequency of TC formation can change on various time scales. In our numerical experiments, the annual frequency of TC formation is held constant.

Fig. 6a shows the simulated changes of the frequency of TC occurrence in the control experiment (E0), in which the

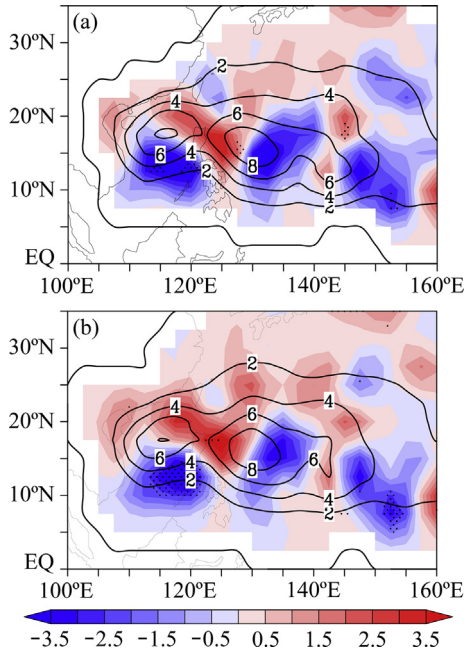

Fig. 5. Spatial distributions of the frequency (contour, unit: 1 per 38 years) of TC formations and its linear trend (shading, unit: 10^{-2} per decade) in TC peak season (June–October) during the period of 1979–2016 for (a) observation from JTWC, (b) random sampling to 705 samples in observation proportion. Results in (b) are divided by a factor of 30. The trend with dots indicates that the value is statistically significant at 90% confidence level.

influences of both of the formation position and environmental steering are included. It can be seen that the simulated changes of TC tracks in the control experiment are in good agreement with the observation (Fig. 4a). The most pronounced feature is the decreasing influence over the SCS. The two prevailing tracks shift westward, increasing the TC influence on the coastal regions of China north of the Taiwan Strait, as suggested by Wu et al. (2005).

Fig. 6b shows the simulated influence of the change of the formation location in E1. TC movements are basically controlled by the mean steering flows in this experiment. Comparing with Fig. 5b, we can find that most of the influence of the track change results from the changes in formation positions. It can be found that the change of the formation location can account for most of the changing trends in Fig. 6a, except the enhancing TC influence along the coastal regions of China north of Taiwan. It is suggested that during the period of 1979–2016 the change of the formation location has played an important role in the observed changes of TC influence in most areas.

Fig. 6c shows the simulated influence of the change of the environmental steering in E2. We can see that the change in the environmental steering also contributes to the decreasing TC activity in the SCS due to the enhanced westerly steering (Fig. 4b), but the influence is relatively smaller than that of the change in the formation location. An important feature is that the change of the environmental steering enhances the TC influence along the southeast coastal regions of China. Our study further confirms previous studies (Wu et al., 2005; Wang and Wu 2013, 2015). The increase of the TC

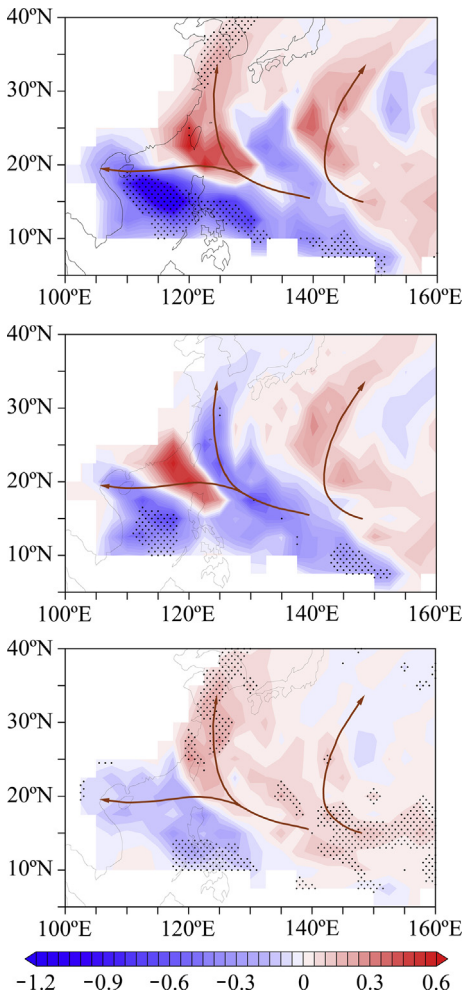

Fig. 6. Linear trend of the frequency of simulated TCs occurrence for (a) E0 (control experiment), (b) E1 (influence of TCs formation location change, and (c) E2 (influence of large−scale steering flow change) in TC peak season (June−October) during 1979−2016. Every year have 705 samples. Results are divided by a factor of 30, unit: per decade. The trend with dots indicates that the value is statistically significant at 90% confidence level. Brown arrows show the climatological typhoon prevailing tracks.

influence caused by the change of steering flows is larger in magnitude than the decrease caused by the change of formation locations along the coastal regions of China to north of Taiwan Island. So the change of steering flows plays an important role in this area.

6. Conclusions

In this study, the Gaussian weight interpolation method is used to calculate the beta drift in the TC track or trajectory model. By simulating historical TC tracks, we find that the improved calculation can better simulate the spatial distribution of the frequency of TC occurrence. The improved track model is further used to understand the TC track change during the period of 1979−2016. Over the past 38 years, the TC activity has been suppressed in the SCS while the TC influence along the southeast coastal regions of China has been increased.

Our sensitivity experiments indicate that the change of the formation location decreases the frequency of TC occurrence in the SCS, Philippine Sea and eastern China, but increases the frequency of TC occurrence in the vicinity of Taiwan Island. The change of the environmental flow exhibits a cyclonic anomalous circulation over southeastern China, decreasing TC influence from the SCS to Philippines but increasing influence in the eastern coastal region of China. Using a previous version of the track model, Zhao and Wu (2014) found that the contribution of the change in the environmental steering is much larger than the change of the formation location. In this study, we find that the change of the formation location plays a dominant role in decreasing TC influence in the SCS while the change of the environmental steering increases the TC influence in the eastern coastal region of China. Note that the trend of TC influence discussed here can include the natural variations on the interdecadal time scale due to the short period used in this study.

Acknowledgments

This research was jointly supported by the National Basic Research Program of China (2015CB452803), the National Natural Science Foundation of China (41730961, 41675051), the Natural Science Foundation for Higher Education Institutions in Jiangsu Province (12KJA170002) and China Special Fund for Metrological Research in the Public Interest (GYGY201506014).

References

Chen, L., Meng, Z., 2001. An overview on tropical cyclone research progress in China during the past ten years. Chin. J. Atmos. Sci. 25 (3), 420−432 (in Chinese).

Colbert, A.J., Soden, B.J., 2012. Climatological variations in North Atlantic tropical cyclone tracks. J. Clim. 25 (2), 657−673.

Emanuel, K., 2008. The hurricane−climate connection. Bull. Am. Meteorol. Soc. 89 (5), ES10−ES20.

Emanuel, K., Ravela, S., Vivant, E., et al., 2006. A statistical deterministic approach to hurricane risk assessment. Bull. Am. Meteorol. Soc. 87 (3), 299−314.

Hall, T.M., Jewson, S., 2007. Statistical modelling of North Atlantic tropical cyclone tracks. Tellus 59A (4), 486−498.

Ho, C.H., Baik, J.J., Kim, J.H., et al., 2004. Interdecadal changes in summertime typhoon tracks. J. Clim. 17 (9), 1767−1776.

Holland, G.J., 1983. Tropical cyclone motion: environmental interaction plus a beta effect. J. Atmos. Sci. 40 (2), 328−342.

Kalnay, E., Kanamitsu, M., Kistler, R., et al., 1996. The NCEP/NCAR 40-year reanalysis project. Bull. Am. Meteorol. Soc. 77 (3), 437−471.

Liu, Z., Zhu, Y., Li, W., et al., 2008. Development of estimating tropical cyclone intensity with meteorological satellite data. J. Trop. Meteorol. 24 (5), 550−556 (in Chinese).

Murakami, H., Wang, B., Kitoh, A., 2011. Future change of western North Pacific typhoons: projections by a 20-km-mesh global atmospheric model. J. Clim. 24 (4), 1154−1169.

Sugg, A.L., 1968. Beneficial aspects of the tropical cyclone. J. Appl. Meteorol. 7 (1), 39−45.

Wang, B., Chan, J.C.L., 2002. How strong ENSO events affect tropical storm activity over the western North Pacific. J. Clim. 15 (13), 1643−1658.

Wang, R., Wu, L., 2013. Climate changes of Atlantic tropical cyclone formation derived from twentieth-century reanalysis. J. Clim. 26 (22), 8995−9005.

Wang, C., Wu, L., 2015. Influence of future tropical cyclone track changes on their basin-wide intensity over the western North Pacific: downscaled CMIP5 projections. Adv. Atmos. Sci. 32 (5), 613−623.

Wang, C., Wu, L., 2016. Interannual shift of the tropical upper-tropospheric trough and its influence on tropical cyclone formation over the western North Pacific. J. Clim. 29 (11), 4203−4211.

Wang, B., Wang, Y., Wu, L., 1998. Dynamics in the tropical cyclone motion: a review. Chin. J. Atmos. Sci. 22 (4), 535−547.

Wang, L., Chen, G., Huang, R., 2009a. Spatiotemporal distributive characteristics of tropical cyclone activities over the Northwest Pacific in 1979−2006. J. Nanjing Inst. Meteor. 32 (2), 182−188 (in Chinese).

Wang, L., Chen, G., Huang, R., 2009b. Quantitative analysis on large scale circulation system modulating landfalling tropical cyclone activities in the diverse Chinese regions. Chin. J. Atmos. Sci. 33 (5), 916−922 (in Chinese).

Wu, L., Wang, B., 2004. Assessing impacts of global warming on tropical cyclone tracks. J. Clim. 17 (8), 1686−1698.

Wu, L., Wang, B., Geng, S., 2005. Growing typhoon influence on. East Asia. Geophys. Res. Lett. 32 (18), 109−127.

Wu, L., Wang, C., Wang, B., 2015. Westward shift of western North Pacific tropical cyclogenesis. Geophys. Res. Lett. 42 (5), 1537−1542.

Yang, Y., Ying, M., Chen, B., 2009. The climatic change of landfall tropical cyclones in China over the past 58 years. Acta Meteorol. Sin. 67 (5), 689−696 (in Chinese).

Yonekura, E., Hall, T.M., 2011. A statistical model of tropical cyclone tracks in the western North Pacific with ENSO-dependent cyclogenesis. J. Appl. Meteor. Climatol. 50 (8), 1725−1739.

Yonekura, E., Hall, T.M., 2014. ENSO effect on East Asian tropical cyclone landfall via changes in tracks and genesis in a statistical model. J. Appl. Meteor. Climatol. 53 (2), 406−420.

Zhang, Q., Liu, Q., Wu, L., 2009. Tropical cyclone damages in China 1983−2006. Bull. Am. Meteorol. Soc. 90 (4), 489−495.

Zhang, J., Wu, L., Zhang, Q., 2011. Tropical cyclone damages in China under the background of global warming. J. Trop. Meteorol. 27 (4), 442−454 (in Chinese).

Zhao, H., Wu, L., 2014. Inter-decadal shift of the prevailing tropical cyclone tracks over the western North Pacific and its mechanism study. Meteorol. Atmos. Phys. 125 (1−2), 89−101.

Zhao, H., Wu, L., Zhou, W., 2009. Observational relationship of climatologic beta drift with large-scale environmental flows. Geophys. Res. Lett. 36 (18), L18809.

Zhao, H., Wu, L., Zhou, W., 2010. Assessing the influence of the ENSO on tropical cyclone prevailing tracks in the western North Pacific. Adv. Atmos. Sci. 27 (6), 1361−1371.

Zhao, J., Wu, L., Zhao, H., 2012. Improvement of tropical cyclone genesis potential index in the western North Pacific Basin. J. Meteor. Sci. 32 (6), 591−599 (in Chinese).